Monthly Notices of the ROYAL ASTRONOMICAL SOCIETY

MNRAS **506,** 3499–3510 (2021) https://doi.org/10.1093/mnras/stab1820
Advance Access publication 2021 July 2

$C_2H_2\cdots CO$ complex and its radiation-induced transformations: a building block for cold synthetic astrochemistry

Pavel V. Zasimov,[1] Sergey V. Ryazantsev [2,1,3,4]★ Daniil A. Tyurin[1] and Vladimir I. Feldman [1]★

[1]*Department of Chemistry, Lomonosov Moscow State University, 119991 Moscow, Russia*
[2]*Center for Energy Science and Technology, Skolkovo Institute of Science and Technology, 121205 Moscow, Russia*
[3]*Moscow Institute of Physics and Technology, Dolgoprudny, 141701 Moscow Region, Russia*
[4]*HSE University, 101000 Moscow, Russia*

Accepted 2021 June 10. Received 2021 June 4; in original form 2021 January 12

ABSTRACT

In this work, we have examined the radiation-induced synthetic chemistry occurring in an astrochemically important C_2H_2–CO system at the molecular level using a matrix isolation approach. The 1:1 $C_2H_2\cdots CO$ intermolecular complex of linear structure was obtained in the solid low-temperature (5 K) noble gas matrices by deposition of the C_2H_2/CO/Ng (Ng = Ar, Kr, Xe) gaseous mixtures and characterized by Fourier-transform infrared spectroscopy. It was found that the X-ray radiolysis of the $C_2H_2\cdots CO$ complex resulted in formation of C_3O (tricarbon monoxide), HCCCHO (propynal), c-H_2C_3O (cyclopropenone), H_2CCCO (propadienone), and HC_3O (oxoprorynyl radical). This means that the studied complex may be considered as the simplest building block (or minimal size of intermolecular reactor) for cold astrochemistry occurring in mixed interstellar ices. Remarkably, the discovered transformations of the complex actually represent synthetic routes leading to various C_3 species, whereas the acetylenic C–H bond cleavage yielding ethynyl radical appears to be a minor process. Prolonged irradiation results in dehydrogenation, while the C_3 skeleton is retained. The interpretation of the $C_2H_2\cdots CO$ radiolysis mechanism (possible reactions pathways) is provided based on the analysis of kinetic curves and matrix effect. Astrochemical implications of the results are discussed.

Key words: astrochemistry – molecular processes – methods: laboratory: solid state – techniques: spectroscopic – ISM: molecules.

1 INTRODUCTION

Acetylene (C_2H_2), one of the simplest hydrocarbons, is believed to play a significant role in the chemistry of the interstellar medium (ISM). It was detected in a variety of objects of the ISM and found to be a rather abundant interstellar molecule. In the gas phase, acetylene was observed around young stellar objects (Lahuis F. & van Dishoeck E. F. 2000; Carr & Najita 2008), in molecular clouds (Lacy et al. 1989), in cometary comae (Mumma et al. 2003; Mumma & Charnley 2011), and Titan's atmosphere (Coustenis et al. 2007). The discovery of acetylene in cometary comae implicitly indicates the possibility of its existence in cometary ice (Cuylle et al. 2014). Furthermore, the gas-phase formation routes cannot entirely account for the abundances of C_2H_2 molecules in space gas (Lahuis F. & van Dishoeck E. F. 2000), which supports the conclusion that acetylene could form in icy media (Kaiser & Roessler 1998) and then sublime into the gas phase. In the icy form, acetylene was found through observation of stars behind molecular clouds (Knez et al. 2008) and on the Titan's surface utilizing Cassini Vims (Singh et al. 2016). The abundance of C_2H_2 (with respect to H_2O) is ca. 0.02 in the interstellar ices (determined from gas-phase observations in Cepheus A east; Sonnentrucker, González-Alfonso & Neufeld 2007) and from 0.001 to 0.01 in cometary comae (Mumma et al. 2003). Thus, one should expect the existence of acetylene in solid-phase generally as a component of ices composed of the most common interstellar molecules (Knez et al. 2012). Carbon monoxide is a major component of various cosmic ices (Whittet et al. 1983, 1985; Tielens et al. 1991) and one may expect C_2H_2 to be a minor but non-negligible component of the CO-based interstellar ices.

Extraterrestrial ices are continuously exposed to various types of irradiations e.g. protons, α-particles, electrons, high-energy photons (Bennett, Pirim & Orlando 2013). It results in modification of their physicochemical properties and, particularly, chemical composition. Roughly speaking, processing of the extraterrestrial ices with the ionizing radiation leads to the breaking of chemical bonds in the source molecules and creation of new bonds and, therefore, formation of new species (Herbst 2017). One should notice that chemistry occurring in the interstellar ices (i.e. in the bulk of icy mantles) under processing with high-energy radiation is considered to be the dominant mechanism of complex organic molecules (COM) formation in the ISM (Öberg 2016; Arumainayagam et al. 2019). Regarding acetylene, it is worth pointing out that C_2H_2 is thought to be an important precursor of larger hydrocarbons, ring molecules, polycyclic aromatic hydrocarbons (PAH) as well as nitriles and cyanopolyynes in the ISM (e.g. Winnewisser & Walmsley 1979; Cherchneff, Barker & Tielens 1992; Balucani et al. 2000; Didriche & Herman 2010; Contreras & Salama 2013; Lukianova et al. 2021). In

★ E-mail: s.ryazantsev@skoltech.ru (SVR); feldman@rad.chem.msu.ru (VIF)

this context, the radiation chemistry of the C_2H_2-containing ices is of particular interest to astrochemists and it has been extensively investigated for several decades. While many works were devoted to pure acetylene ices (Abplanalp & Kaiser 2020; Pereira et al. 2020; and references therein), and acetylene in water-dominant ices (Wu et al. 2002; Hudson & Moore 2003; Hudson & Loeffler 2013 and references therein), the studies of radiation-induced chemistry in the C_2H_2–CO ices are rather limited (Zhou et al. 2008; Abplanalp & Kaiser 2019).[1]

The processing of the mixed ices of acetylene and carbon monoxide with 5 keV electrons at 10 K (Zhou et al. 2008) results in the formation of cyclopropenone (c-H_2C_3O), propynal (HCCCHO), formyl radical (HCO), vinylacetylene ($HCCC_2H_3$), propadienone (H_2CCCO), C_3O, C_5O, and C_3O_2 as it was determined by Fourier-transform infrared (FTIR) spectroscopy (to note, four latter species were assigned only tentatively). In addition, several absorption features observed in the FTIR spectra were assigned to specific functional groups (e.g. C–H_{str}, C=C_{str}, and C=O_{str}), but not to individual molecular carriers. Formation of cyclopropenone and propynal was confirmed by mass spectrometric analysis. Based on analysis of temporal profiles of c-H_2C_3O and HCCCHO accumulation and ab initio calculations Zhou et al. (2008) suggested that the former species could be synthesized via an addition of triplet CO to C_2H_2 (or vice versa), while the latter one could be formed from the 1:1 C_2H_2···CO complex through the creation of a [C_2H···HCO] caged radical pair followed by its recombination. Abplanalp & Kaiser (2019) revisited the radiation chemistry induced in the low-temperature mixed C_2H_2–CO ices utilizing the FTIR spectroscopy and tunable photoionization reflectron time-of-flight mass spectrometry. It was confirmed that irradiation of the mixed C_2H_2–CO ices at 5 K with 5 keV electrons led to the formation of c-H_2C_3O and HCCCHO. In addition to these species, such molecules as ketene (H_2CCO), ethynol (HCCOH), propenal (CH_2CHCHO), propanal (CH_3CH_2CHO), acetone (CH_3COCH_3), and glyoxal (CHOCHO) were tentatively detected in the samples after irradiation. Thus, the radiation chemistry in the C_2H_2–CO system leads to a variety of complex organic species of potential prebiotic importance.

Despite the recent progress in the field of laboratory simulations of the radiation-driven processes in the astrochemically relevant ices, comprehensive understanding of the mechanisms of such processes is lacking. This gap mainly results from poor knowledge on the nature of reactive intermediates lying on the pathways of chemical transformation from the source molecules to the products. In fact, the studies of radiation-induced processes in the astrochemically relevant ices often cannot provide information about the primary reaction intermediates owing to several reasons. First, the intermediate species are typically highly reactive and they decay in ices before the measurement, even at the lowest temperatures. Secondly, the spectroscopic identification of intermediate species may be obscured due to overlapping with intense absorption of parent substance and severe line broadening caused by strong interaction with a medium. Thirdly, high (astrochemically relevant) absorbed doses typically used in these experiments may result in the secondary radiation-induced transformations of primary intermediates. A matrix isolation approach has proven to be an efficient way to resolve these issues, which makes it a very valuable complementary method to study the radiation-induced processes in the icy media (Feldman et al. 2016; Ryazantsev; Zasimov & Feldman 2018; Zasimov et al. 2020a).

[1]When the manuscript was under review, we became aware of the new study related to this system (Kleimeier et al. 2021).

Indeed, the matrix isolation technique implies an isolation of the studied species in the solid low-temperature inert media (typically, solid noble gases). The inertness of a surrounding medium prevents the loss of highly reactive intermediates in chemical reactions with the environment. Moreover, it reduces the chemical complexity of a system that allows one to focus on key processes of the radiation-induced transformations. At the same time, the low perturbation of isolated species by a matrix and transparency of noble gases for electromagnetic radiation over a wide range significantly facilitates the detection of intermediate species. It is worth noting that matrix isolation was widely applied to characterize astrochemically important intermediates for several decades (Allamandola 1987; Zack & Maier 2014).

An approach to mechanistic studies of the processes involved in ice astrochemistry through matrix isolation developed in our group (Feldman et al. 2016) is based on the concept that matrix can be considered as a model medium (or reservoir) for chemical processing of the isolated molecules in focus or their small associates under the action of ionizing radiation. Even though solid noble gases are not chemically relevant to the cosmic ices, they can provide a valuable insight into the mechanisms of the radiation-induced processes in the low-temperature solids and probably represent perfect model media to investigate the general effect of a solid medium on such processes. In this case, the energy is primarily absorbed by a chemically inert matrix and then effectively migrates to a studied molecule resulting in its ionization or excitation, which makes it possible to explore the effect of matrix physical characteristics (such as ionization energy and polarizability) on the chemical reactions of the resulting states of the guest species. Furthermore, high efficiency of energy transfer in the case of noble gases allows us to trace the step-by-step radiation-driven evolution of a system under consideration. Indeed, high conversion (up to $>$ 90 per cent) of parent species may be achieved using moderate absorbed doses of X-rays (up to hundreds kGy). This actually implies a very useful opportunity of accelerated simulation in the laboratory time-scale. Such approach ('matrix isolation for astrochemistry') was previously applied to characterize the radiation-induced transformations of a number of simple astrochemically important molecules isolated in noble gas matrices (Ryazantsev & Feldman 2015b; Feldman et al. 2016; Kameneva, Tyurin & Feldman 2016a; Saenko & Feldman 2016; Kameneva, Volosatova & Feldman 2017b; Ryazantsev et al. 2018; Lukianova, Sanochkina & Feldman 2019; Volosatova, Kameneva & Feldman 2019; Lukianova et al. 2020). Using X-rays for such simulation is generally justified by the fact that the chemical effects are predominantly induced by secondary electrons (up to $>10^3$ secondary electrons are formed per an absorbed primary photon). Thus, we believe that the type and energy spectrum of applied radiation is not crucial as we are focusing on the qualitative description of the basic mechanism of chemical transformations (note that no qualitative difference was found between the chemical transformations of matrix isolated molecules induced by fast electrons and X-rays; Feldman 1999; Feldman et al. 2016).

It is important to note that matrix isolation can also be applied to simulation of synthetic astrochemical processes, if we start from intermolecular complexes instead of single isolated molecules in matrices. Considering the present context, the 1:1 complexes represent the simplest building blocks for synthetic astrochemistry. Recently, this concept was used in our laboratory to investigate the radiation-driven chemistry of astrochemically relevant complexes, such as H_2O···CO_2, HCN···CO_2, HCN···CO, C_2H_2···H_2O, H_2O···CO, and C_2H_n···HCN ($n = 2, 4, 6$) (Ryazantsev & Feldman 2015a; Kameneva et al. 2016b; Kameneva, Tyurin & Feldman 2017a; Ryazantsev,

Zasimov & Feldman 2020; Zasimov et al. 2020; Lukianova et al. 2021). In particular, it was found that some of these systems could provide the key to better understanding the synthetic routes, which may lead to formation of complex organic molecules and prebiotic evolution, such as formation of HOCO radical and formic acid (Ryazantsev & Feldman 2015a; Ryazantsev et al. 2020), simple nitriles and isonitrliles (Lukianova et al. 2021). It was shown that the radiolysis of the C_2H_2···H_2O complex (Zasimov et al. 2020) resulted in formation of ketene (H_2CCO), ketenyl radical (HCCO), vinyl alcohol (CH_2CHOH), CO (carbon monoxide), and CH_4 (methane). All these products were actually identified in the studies of irradiated ices (Wu et al. 2002; Hudson & Moore 2003; Hudson & Loeffler 2013), but the mechanism of their formation was not deduced from the experiments in complex ices, so the matrix isolation results were quite informative in this aspect. Generally speaking, such approach provides substantially new opportunities to investigate the mechanisms of chemical reactions occurring in low-temperature mixed ices.

The C_2H_2···CO complexes should be among the key building blocks in synthetic astrochemistry both because the abundance of their components and because of diversity of their possible transformations. In this work, we report the results of the FTIR studies of the X-rays radiation-induced transformations of the 1:1 C_2H_2···CO complex isolated in solid noble gas matrices (Ar, Kr, and Xe) at 5 K and discuss their possible implications to astrochemistry.

2 EXPERIMENTAL DETAILS

Acetylene ($^{12}C_2H_2$, 99.6 per cent, SIAD; $^{13}C_2H_2$, 99.6 per cent, 99 per cent at. ^{13}C, Aldrich), carbon monoxide (CO, 98 per cent, MGPZ), argon (Ar, 99.9995 per cent, Voessen), krypton (Kr, 99.9998 per cent, Akela-N), and xenon (Xe, 99.9994 per cent, Medxenon) were used as purchased. Gaseous mixtures acetylene/carbon monoxide/noble gas (acetylene = $^{12}C_2H_2$ or $^{13}C_2H_2$; noble gas = Ar, Kr, or Xe; mixing ratio was 1/1÷3/1000) were prepared by standard manometric procedure and then used in the matrix isolation experiments. Acetylene/noble gas 1:1000 mixtures were used in complementary experiments. The matrix-isolation experiments were conducted utilizing an original closed-cycle helium cryostat based on a SHI RDK-101E cryocooler. The detailed description of the used experimental setup can be found elsewhere (Feldman 2014). The pressure inside the cryostat chamber prior to the experiment was less than 10^{-4} Torr. Gaseous mixtures were slowly (ca. 2 mmol h^{-1} per 1 cm^2 of the KBr substrate) deposited on to a cooled KBr substrate. The temperature of the substrate was controlled by a Lakeshore 325 temperature controller connected to the calibrated Cernox™ temperature sensor. The temperature of the substrate during deposition was specially adjusted to obtain low-scattering samples containing sufficient amount of the 1:1 C_2H_2···CO complexes (typically, it was 17, 25, and 34 K for Ar, Kr, and Xe matrices, respectively). Measuring FTIR spectra provided the real-time monitoring of the content, thickness, and transparence of the matrices being deposited. The deposition was stopped after obtaining ca. 60–100 μm thick matrices. The obtained matrix samples were slowly cooled down to 5 K (minimal available temperature) and then irradiated with X-rays (through a 45 μm aluminium foil window mounted in the cryostat) from a 5BKhV-6(W) X-ray tube with a tungsten anode (45 kVp, anode current 80 mA, effective X-ray energy is ca. 20 keV). The absorbed dose rate in the matrix samples was estimated in our earlier work (Zasimov et al. 2020b); the values are 38.6, 72.9, and 55.0 Gy s^{-1} for Ar, Kr, and Xe, respectively (in case of 80 μm thick matrices – typical sample thickness used in our experiment). The irradiation time varied from 1 to 120 min, so the samples were X-irradiated up to different absorbed doses (from 2 to 525 kGy, typically 5–7 points in each experiment).

The FTIR spectra of the matrices were recorded in the 7000–450 cm^{-1} range at 5 K using a Bruker Tensor II spectrometer equipped with a cooled MCT detector (resolution of 1 cm^{-1}, averaging over 144–500 scans). The normalized concentrations of isolated species in a given matrix sample were obtained by normalization of absorption intensity of a selected spectral band to a maximum corresponding value achieved in the experiment. Relative uncertainty of the integrated infrared absorption values was estimated to be ca. 3 per cent which gives relative error of ca. 4.3 per cent for the normalized concentration values, as determined using the variance formula (Ku 1966).

3 RESULTS AND DISCUSSION

3.1 Preparation and identification of the C_2H_2···CO complexes in low temperature noble gas matrices

The C_2H_2···CO complex has been previously investigated using supersonic slit jet technique and characterized by microwave spectroscopy (Germann, Tschopp & Gutowsky 1992; and references therein) and FTIR spectroscopy in the regions of C–H_{str} (Marshall, Prichard & Muenter 1989; Hünig, Oudejans & Miller 2000; and references therein), and C≡O_{str} (Kawashima & Nishizawa 1996; Rivera-Rivera et al. 2012; Barclay et al. 2018) vibrations. A linear HCCH···CO structure was observed experimentally, and this structure is the most stable configuration of the complex according to the theoretical predictions (Adamowicz 1992; Rivera-Rivera et al. 2012; and references therein). Although matrix isolation technique is widely applied to the studies of various intermolecular complexes (Young 2013; Khriachtchev 2015), we are unaware of any reports on the C_2H_2···CO complexes in low-temperature matrices.

Binary intermolecular complexes in low-temperature matrices might be prepared in two different ways: (i) deposition of a mixture containing both components of the target complex; (ii) photo- or radiation-induced dissociation of an appropriate matrix-isolated molecular precursor. The latter way usually provides quite high yields of the target complexes, as was shown, e.g. for the H_2O···CO and C_2H_2···CO_2 complexes produced via *UV*-photolysis of matrix-isolated HCOOH and HCCCOOH, respectively (Khriachtchev 2015). However, when one aims to study in detail the radiation chemistry of a given matrix-isolated complex, such preparation approach seems to be non-preferred, because it provides matrix samples containing multiple side compounds such as alternative (non-targeted) complexes, secondary photolysis products as well as residual amounts of precursors. Thus, it is hardly possible to distinguish the radiation-induced transformations of the target complex from the complicated set of various processes occurring under the radiolysis of matrix samples with diverse chemical compositions. On the other hand, the preparation of matrix-isolated X···Y complexes via the deposition of X/Y/Ng mixtures (Ng = noble gas) has been shown to be practically efficient in our previous studies (Kameneva et al. 2017a; Ryazantsev et al. 2020; Zasimov et al. 2020a; Lukianova et al. 2021). Other species detected in matrix samples obtained using this approach are the agglomerates $(X)_n$, $(Y)_n$, and $(X)_n$···$(Y)_m$ (n or $m \geq 2$) and the optimization of the experimental parameters (concentrations of the components in a gaseous mixture, deposition temperature, etc.) might be performed in order to maximize the relative amount of the target 1:1 X···Y complexes (and minimize the amount of undesirable agglomerates). In the case of the C_2H_2···CO

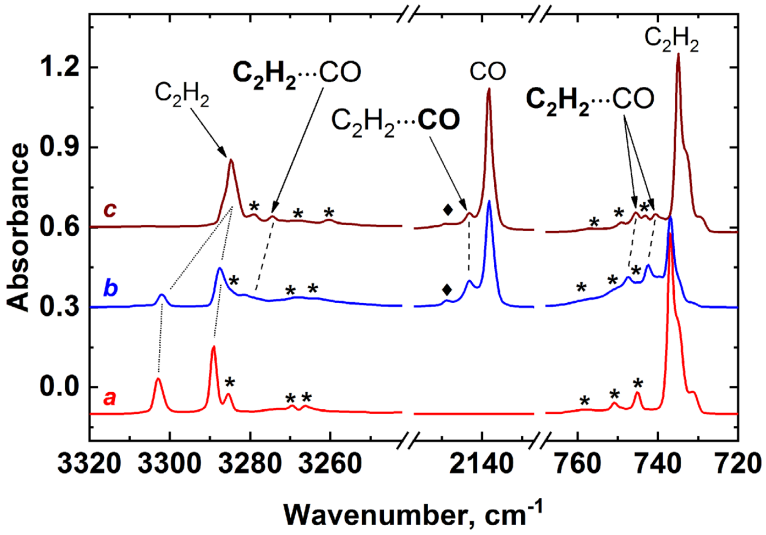

Figure 1. Fragments of the FTIR spectra of the deposited matrices: (a) $^{12}C_2H_2$/Ar 1:1000; (b) $^{12}C_2H_2$/CO/Ar 1:3:1000; (c) $^{13}C_2H_2$/CO/Ar 1:3:1000. Absorptions of $(C_2H_2)_n$ associates are marked with asterisks. Absorptions of H_2O···CO complexes (impurity) are marked with diamonds.

complexes studied in this work, we found that increase of CO concentration (from common 1:1000 ratio to 3:1000, with respect to Ng) enlarged the amount of the target 1:1 C_2H_2···CO complex in the matrix samples. Further increase of CO concentration would lead to efficient formation of larger C_2H_2···$(CO)_n$ associates, while increase of C_2H_2 concentration would yield higher amount of the undesirable $(C_2H_2)_n$ and $(C_2H_2)_n$···CO agglomerates. It is worth noting that the formation of $(CO)_n$ agglomerates in low-temperature matrices is inefficient due to the low energy of CO···CO intermolecular interaction (Dawes, Wang & Carrington 2013). One should also bear in mind that the temperature choice may be also a tricky thing – while the relatively low deposition temperatures provide 'mostly monomeric' samples (moreover, usually, with poor optical quality), the use of higher temperatures increases not only the yield of a target 1:1 complex, but the amount of larger agglomerates as well. To note, the optimal deposition temperature particularly depends on matrix material – see values given in the Experimental Details section.

The FTIR spectra of deposited $^{12}C_2H_2$/CO/Ng (Ng = Ar, Kr, and Xe) matrices reveal strong absorptions of CO and $^{12}C_2H_2$ isolated molecules as well as absorption bands of acetylene dimers and trimers (Dubost 1976; Golovkin et al. 2013; Ryazantsev et al. 2018). Trace amounts of water and carbon dioxide (typical IR active atmospheric impurities) and the H_2O···CO and $^{12}C_2H_2$···H_2O complexes were also found (Zasimov et al. 2020a; Ryazantsev et al. 2020). Weak signals of ^{13}CO were detected as well (natural abundance of ^{13}C isotope is ca. 1 per cent). In addition to these absorption bands, new features were detected in the FTIR spectra of the studied matrices (example of an Ar matrix is presented in Fig. 1, spectra of $^{12}C_2H_2$/CO/Kr and $^{12}C_2H_2$/CO/Xe deposited matrices are demonstrated in Fig. S1). These features found in the spectral regions of C_2H_2 and CO vibrations have characteristic shifts from the corresponding monomeric absorptions (Table 1) and they were attributed to the 1:1 $^{12}C_2H_2$···CO complex. As could be seen from Table 1, the absorptions of the complex in the noble gas matrices have a characteristic red shift (from − 10.6 to − 11.5 cm^{-1} in different matrices) and blue shift (from +4.9 to +10.2 cm^{-1}) in the C–H_{str} and C≡O_{str} regions, respectively. These values are in good agreement with the shifts of −9 cm^{-1} and +6.0 cm^{-1}, respectively, observed previously for the HCCH···CO complex in gas-phase (Marshall et al. 1989; Kawashima & Nishizawa 1996). For the CCH_{bend} mode, the complexation-induced blue shift (from +6.4 to +14.0 cm^{-1} in different matrices) was observed in our experiments. Worth noting, in the case of Ar and Kr matrices, two CO-induced bands were detected in the CCH_{bend} region, and that probably evidence stabilization of the C_2H_2···CO complex in two different matrix sites. We may notice that multiple bands are typically observed for the CCH_{bend} absorptions of C_2H_2 molecules and its complexes isolated in low-temperature matrices (Zasimov et al. 2020a; Jovan Jose et al. 2007; Ryazantsev et al. 2018). Complementary experiments with $^{13}C_2H_2$/CO/Ar matrices were performed to confirm the assignment; the corresponding spectrum is also given in Fig. 1. Similarity of the complexation-induced shifts observed in acetylene-^{12}C and acetylene-^{13}C samples (see Table 1) supports our experimental assignment of the C_2H_2···CO complexes. The computed complexation-induced shifts for the $^{12}C_2H_2$···CO and $^{13}C_2H_2$···CO complexes (in the linear HCCH···CO structure) provided in Table 1 shows reasonable agreement with the experimental results. (The details and results of our computational study of the C_2H_2···CO complexes will be published elsewhere.)

An interesting observation is that both components of the Fermi resonance doublet of the $^{12}C_2H_2$ monomers in the $^{12}C_2H_2$/CO/Ng 1:1:1000 matrices are slightly red-shifted (ca. −0.3, −0.1, −0.2 cm^{-1} and − 0.7, −0.1, −0.3 cm^{-1} for the high- and low-frequency components, respectively; Ng = Ar, Kr, and Xe) in comparison to their positions observed in corresponding $^{12}C_2H_2$/Ng 1:1000 matrices. Furthermore, this shift increases with increase of CO concentration: in the $^{12}C_2H_2$/CO/Ng 1:3:1000 matrices, the corresponding values are ca. −0.8, −0.2, −0.3 cm^{-1} and −1.3, −0.2, −0.4 cm^{-1} for high- and low-frequency components, respectively. The C–H_{str} absorption of $^{13}C_2H_2$ monomers in $^{13}C_2H_2$/CO/Ar matrices (to note, Fermi resonance is lifted in the $^{13}C_2H_2$ molecules) is also slightly redshifted, but the shift value (ca. −0.3 cm^{-1} both for the 1:1:1000 and 1:3:1000 samples) seems to be independent of CO concentration, probably due to Fermi resonance lifting. Meanwhile, we did not detect noticeable CO-induced shifts for any other absorption of monomeric C_2H_2 in the C_2H_2/CO/Ng matrices. The effect of drifting of acetylene IR absorptions was reported earlier (Jovan Jose et al. 2007) for $^{12}C_2H_2$ molecules isolated in mixed Ar/N_2 matrices even at low N_2 concentrations (C_2H_2/N_2/Ar 1:1:1000 samples). It is worth noting

Table 1. Absorption maxima of the $^{m}C_2H_2$...^{12}CO (m = 12, 13) complex, $^{m}C_2H_2$ and ^{12}CO isolated molecules and the corresponding complexation-induced shifts (cm^{-1}) in Ar, Kr, and Xe matrices. Additional features due to site splitting are provided in italic. Complexation-induced shifts corresponding to less intense absorption features of the C_2H_2···CO complex (measured from the principal absorption of monomeric acetylene) are also provided in italic. Unperturbed positions of (ν_3) C_2H_2 band ($\nu_3{}^0$) calculated as described elsewhere (Rutkowski et al. 2002) and corresponding complexation-induced shifts are provided in parentheses. The complexation-induced shifts predicted by the CCSD(T)/L3a_3 computations are given for comparison.

Assignment	Experimental data										Computed complexation-induced shifts	
	$^{12}C_2H_2/^{12}CO$ Ar			$^{12}C_2H_2/^{12}CO$ Kr			Xe		$^{13}C_2H_2/^{12}CO$ Ar			
	Complex	Monomer	Shift	Complex	Monomer	Shift	Complex	Monomer	Shift	Complex	Monomer	Shift	$^{12}C_2H_2$...^{12}CO	$^{13}C_2H_2$...^{12}CO
C_2H_2 (ν_3)	–	3302.0*	–	–	3293.1*	–	–	3280.1*	–	–	–	–	–	–
	–	*3287.6**	–	–	3280.0*	–	–	3266.4*	–	–	–	–	–	–
	3281.5	(3292.3)	**(−10.8)**	3276.6	(3287.2)	**(−10.6)**	3261.2	(3272.7)	**(−11.5)**	3274.4	3284.7	**−10.3**	**−9.8**	**−9.9**
C_2H_2 (ν_5)	747.4	736.9	**+10.5**	739.0	732.6	**+6.4**	741.6	727.6	**+14.0**	745.5	735.0	**+10.5**	**+18.5**	**+18.4**
	742.5	*734.8sh*	***+5.6***	736.3	–	**+3.7**	–	–	–	740.6	*732.9sh*	***+5.6***	–	–
	–	*731.3*	–	–	–	–	–	–	–	–	*729.3*		–	–
CO (ν_1)	2143.1	2138.2	**+4.9**	2140.9	2135.8	**+4.9**	2143.4	2133.2	**+10.2**	2143.1	2138.2	**+4.9**	**+8.6**	**+8.6**

Notes. sh – shoulder. ∗Fermi resonance (ν_3, ν_{2+4+5}).

that the value and the direction of the C–H_{str} band shift as well as its dependence on dopant concentration (value of red-shift grows with increasing the N_2 content) are very similar to those observed in this work. Furthermore, the position of the CCH_{bend} absorption (that is not suffering from Fermi resonance) was less affected than that of the C–H_{str} one. These observations were explained by perturbation of the electronic structure of C_2H_2 molecule due to replacement of some surrounding Ar atoms by N_2 molecules (Jovan Jose et al. 2007). We believe that similar effect observed in the C_2H_2/CO/Ng matrices could be treated in the same way since the basic molecular properties (size, electronic structure, polarizability) of CO and N_2 molecules are quite similar.

3.2 Radiation-induced transformations of the matrix-isolated C_2H_2···CO complexes

The radiolysis of deposited matrices resulted in decomposition of both monomeric acetylene and C_2H_2···CO complex with simultaneous formation of new species (see Fig. 2). Matrix-isolated CO molecules do not decompose under X-radiolysis (Kameneva et al. 2017a). However, 'hot' hydrogen atoms produced upon radiolysis of H-containing molecules may react with CO molecules in matrices yielding HCO radicals. Absorptions of HCO radicals (2482.6, 1863.2, and 1085.7 cm^{-1}; 2466.8, 1860.3, and 1081.2 cm^{-1}; 2442.7, 1856.7, and 1076.4 cm^{-1} in Ar, Kr, and Xe, respectively (Milligan & Jacox 1969) appear in the C_2H_2/CO/Ng matrices after irradiation with X-rays. Radiolysis of isolated acetylene molecules was studied in our earlier work (Ryazantsev et al. 2018). C_2H_2 undergoes a stepwise dehydrogenation under radiolysis resulting in the formation of C_2H and C_2 species. The former species was detected in the irradiated C_2H_2/CO/Ng matrices (Ng = Ar, Kr, and Xe) while the latter one was detected only in a Xe matrix (C_2 vibration becomes IR active due to complexation with a Xe atom; Maier & Lautz 1998). These products result from isolated acetylene molecules. Dissociation of C_2H_2 molecules complexed with another species may lead to formation of a complex of C_2H radical, which may be identified by characteristic vibronic absorptions shifted from those of monomeric C_2H. (Ryazantsev et al. 2017 reported comparative investigation of the vibronic spectra of monomeric and complexed C_2H radical in low-temperature matrices.) The comparison of X-irradiated C_2H_2/CO/Ng and C_2H_2/Ng matrices in the corresponding spectral region is presented in Fig. S2, SI. In a Xe matrix, the absorptions of C_2H are too broad to be analysed. In a Kr matrix, the same set of vibronic bands was observed for both CO-doped and CO-free matrices, and that gives no evidences for a possible formation of C_2H···CO. In C_2H_2/CO/Ar matrices, main vibronic bands of C_2H seem to have some satellites, although the low overall intensity of these bands did not allow us to perform a detailed spectroscopic analysis and make reliable assignment of the satellite absorptions (in fact, shoulders of the main ones). To note, the overall yield of C_2H in C_2H_2/CO/Ar matrices was evidently lower as compared to those in the CO-free C_2H_2/Ar matrices. Absorption of C_2H^- species (1768.6 and 1716.3 cm^{-1} for the $^{12}C_2H^-$ and $^{13}C_2H^-$, respectively (Forney, Jacox & Thompson 1992; Andrews et al. 1999) was additionally observed in an Ar matrix (higher yield in CO-doped samples) but it was not detected in Kr and Xe matrices. To the best of our knowledge, there are no reports on the formation of C_2H^- anions in Kr and Xe matrices. Signals of solvated proton (Ar_2H^+, Kr_2H^+, and Xe_2H^+) were observed as well (Kunttu & Seetula 1994). Weak signals of C_2H_3 and C_4 products which result from radiolysis of $(C_2H_2)_2$ dimers were detected (Ryazantsev et al. 2018). Traces of

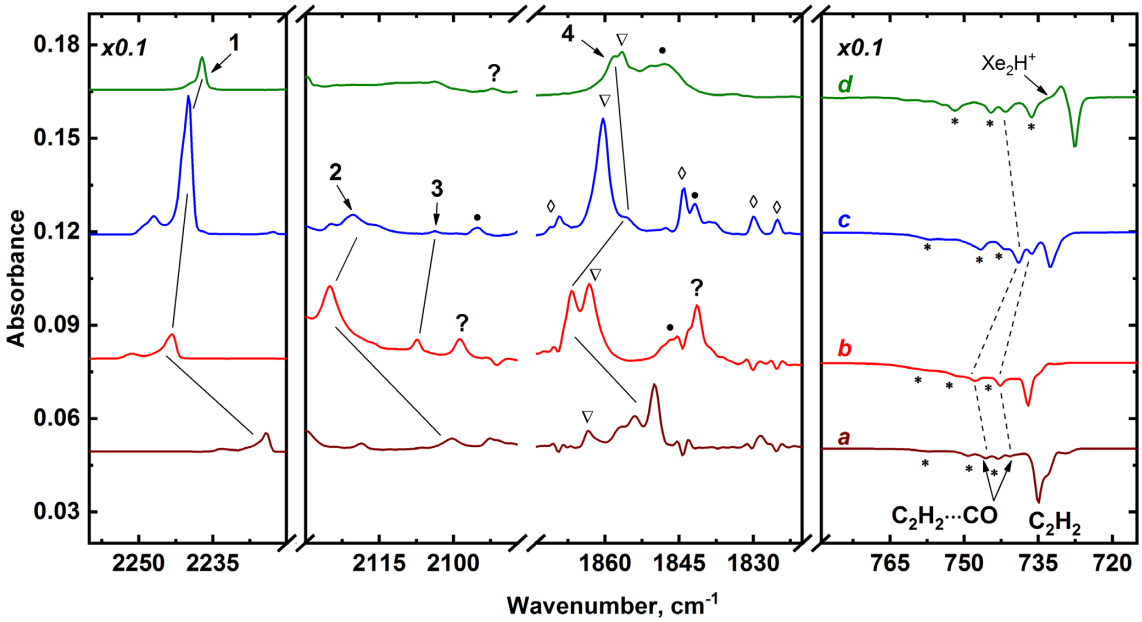

Figure 2. Fragments of the difference FTIR spectra of the $^{13}C_2H_2$/CO/Ar (a), $^{12}C_2H_2$/CO/Ar (b), $^{12}C_2H_2$/CO/Kr (c), and $^{12}C_2H_2$/CO/Xe (d) matrices showing the result of irradiation with X-rays. Each spectrum represents the sample irradiated to a maximum dose in the experiment. The following radiolysis products isomers are marked with digits: C_3O (1), H_2CCCO (2), HCCCHO (3), and c-H_2C_3O (4). Absorptions due to HCO and C_2H are marked with a triangle and a bullet, respectively. Absorptions due to $(C_2H_2)_n$ are marked with asterisks. The non-matrix absorptions due to atmospheric water are marked with diamonds. Note that the spectra in the left-hand and the right-hand panels and are multiplied by the factor 0.1.

the radiolysis products of the $H_2O\cdots CO$ and $C_2H_2\cdots H_2O$ complexes were also identified (Ryazantsev et al. 2020; Zasimov et al. 2020a).

In addition to the absorptions of the abovementioned species, the FTIR spectra of $^{12}C_2H_2$/CO/Ng matrices irradiated with X-rays reveal the appearance of new features which originates from the radiolysis products of the $^{12}C_2H_2\cdots CO$ complex (Fig. 2). These new features were attributed to tricarbon monoxide (C_3O, weak signals of its isotopomers were detected as well as due to natural abundance of ^{13}C), oxoprorynyl radical (HC_3O, weak signals in all studied matrices), propynal (HCCCHO), propadienone (H_2CCCO), and cyclopropenone (c-H_2C_3O). It is worth noting that all of these products were found in Ar and Kr matrices while only C_3O, HC_3O, and c-H_2C_3O were detected in an Xe matrix. The complementary experiments with $^{13}C_2H_2$/CO/Ar matrices provide support for these observations: radiolysis of the $^{13}C_2H_2\cdots CO$ complex in an Ar matrix results in the formation of $^{13}C^{13}C^{12}CO$ (weak signals of its isotopomers were detected as well due to natural abundance of ^{13}C and ^{12}C-impurity in $^{13}C_2H_2$), $H^{13}C^{13}C^{12}CHO$, $H_2{}^{13}C^{13}C^{12}CO$, c-$H_2{}^{13}C^{13}C^{12}CO$, and weak signal of $H^{13}C^{13}C^{12}CO$ (Fig. 2). The absorption bands of the abovementioned products are summarized in Table 2. Unassigned radiation-induced absorption bands are listed in Table S1. Absorptions of C_3O and its isotopomers in Ar and Xe matrices were attributed using the data from previous matrix-isolation studies (Brown et al. 1985; Botschwina & Reisenauer 1991; Maier & Lautz 1998), while the corresponding bands in Kr matrix were assigned considering reasonable matrix shifts. The higher frequency component observed for the $C=O_{str}$, $CCCO_{asym\ str}$, and $CCCO_{bend}$ absorptions of C_3O can belong to the C_3O–H_2 molecular pairs trapped within the same matrix cage (similar to the case of H_2CCO–H_2 molecular pairs reported earlier by Zasimov et al. 2020a). The $^{13}C^{13}C^{12}CO$ absorption corresponding to the $CCCO_{asym\ str}$ mode is rather weak and overlaps with intense signal attributed to c-$H_2{}^{13}C^{13}C^{12}CO$, thus this particular band was not detected in the X-irradiated $^{13}C_2H_2$/CO/Ar matrices. HCCCHO absorptions in an argon matrix were assigned according to the previous report (Szczepanski, Ektern & Vala 1995); the corresponding signals in a Kr matrix (assigned considering reasonable matrix shifts) were less intense and the $C=O_{str}$ absorption of propynal was not reliably detected in the latter case. Absorption at 2125.0 cm^{-1} in Ar matrix (2120.8 cm^{-1} in Kr) was attributed to H_2CCCO, according to the gas-phase measurements (value of 2127.1 cm^{-1} was reported by O'Sullivan et al. 2007) and argon matrix-isolation studies (Chapman, Miller & Pitzenberger 1987). We may note that Chapman et al. (1987) ascribed 14 absorption bands to propadienone in Ar matrix (obtained by pyrolysis of diazotetronic acid) without vibrational modes assignment, while bands with maxima at 2177 and 2125 cm^{-1} (relative intensity ca. 1:5) were much more intense than others. However, according to calculations of East (1998), the 2177 cm^{-1} absorption is not a fundamental of propadienone. Moreover, lactoketene which is also a product of the diazotetronic acid pyrolysis, absorbs at 2176 cm^{-1} in Ar marix (Chapman et al. 1987). Thus, we believe that the 2177 cm^{-1} absorption might be erroneously ascribed to propadienone in Ar matrix. We did not observe this band in our experiments, but reliably detect H_2CCCO by its most intense absorption at 2125.0 cm^{-1} (all the other absorptions are too low-intensive to be observed). In a Kr matrix, the 2120.8 cm^{-1} absorption was ascribed to propadienone. Taking into account the expected shift due to isotopic substitution, two absorptions (with maxima at 2118.6 and 2100.5 cm^{-1}) observed in the irradiated $^{13}C_2H_2$/CO/Ar matrix could be considered for assignment to $H_2{}^{13}C^{13}C^{12}CO$. Analysis of accumulation kinetics (see the text below) favours the 2100.5 cm^{-1} feature to be attributed to $H_2{}^{13}C^{13}C^{12}CO$ (this absorption band showed kinetic behaviour, which agreed with propadienone accumulation profile in the $^{12}C_2H_2$/CO/Ar). Thus, we tentatively assign the absorption at 2100.5 cm^{-1} to $H_2{}^{13}C^{13}C^{12}CO$ isolated in Ar matrix. Absorptions of cyclopropenone observed in our experiments were

Table 2. Absorption maxima (cm^{-1}) of the C_2H_2···CO complex radiolysis products in Ar, Kr, and Xe matrices. Tentative assignments are in italic.

Species	Assignment	$^{12}C_2H_2$···CO			$^{13}C_2H_2$···CO	Ref.
		Ar	Kr	Xe	Ar	
C_3O	$C=O_{str} + CCCO_{bend}$ $C=O_{str}$	3174.8	3169.5	3165.7	*3135.6*	Botschwina & Reisenauer (1991); Brown et al. (1985); Maier & Lautz (1998)
	–	2251.4	2249.1sh	2239.7sh	2232.2	–
	–	2247.0 sh	2246.9	2237.2	2226.2 sh	–
	–	2243.3	2239.9		2224.1	–
	[a]	2240.0	2237.0	2234.8	2240.0	–
	[b]	2225.7	2222.7	2220.7	2225.7	–
	[c]	2194.4	2190.7	2187.9	–	–
	[d]	–	–	–	2173.6	–
	$CCCO_{asym\ str}$	1908.7	1908.2	1904.4	–	–
	–	1907.3	1905.8	–	–	–
	$CCCO_{bend}$	579.4	577.1	574.4	575.6	–
HC_3O	$CCCO_{asym\ str}$	2308.6	*2304.6*	*2299.3*	2297.3	Jiang & Graham (1993)
HCCCHO	$C{\equiv}C_{str}$	2107.3	2103.9	–	2035.0	Szczepanski et al. (1995)
	$C=O_{str}$	1688.1	–	–	*1686.9*	–
	$C–C_{str}$	940.1	937.2	–	929.9	–
H_2CCCO	CO_{str}	2125.0	2120.8	–	*2100.5*	Chapman et al. (1987); East (1998); O'Sullivan et al. (2007)
c-H_2C_3O[i]	CO_{str}	*1875.2*	*1856.2*	*1858.0*	*1856.5*	Brown et al. (1975)
	–	*1872.4*	–	–	*1854.0*	–
	–	1866.6	–	–	1850.1	–
	$C–C_{str}$	1135.6	–	–	1113.6	–
	$C–H_{wag\ in\text{-}plane}$	829.4	–	–	823.6	–

Notes. The main set of C_3O absorptions is provided for $^{12}C^{12}C^{12}CO$ ($^{12}C_2H_2$···CO) and $^{13}C^{13}C^{12}CO$ ($^{13}C_2H_2$···CO) isotopomers. $^{13}C^{12}C^{12}CO$[a]; $^{12}C^{13}C^{12}CO$[b]; $^{12}C^{12}C^{13}CO$[c]; $^{13}C^{13}C^{13}CO$[d] isotopomer signal. In the $^{13}C_2H_2$/CO/Ar system the weak signal of $^{12}C^{13}C^{12}CO$ species overlaps with intense signal of $^{13}C^{13}C^{12}CO$ isotopomer.

assigned according to the gas-phase (1883 cm^{-1}, $C=O_{str}$ mode) and solid-phase (1856, 1180, and 871 cm^{-1} for $C=O_{str}$, $C–C_{str}$, and $C–H_{wag\ ip}$ modes, respectively) data reported by Brown et al. (1975). The $C=O_{str}$ absorption of c-H_2C_3O in Ar matrix shows complex structure, presumably due to site splitting effect. Signal of HC_3O (2308.0 cm^{-1}) was attributed according to the previous argon matrix isolation experiments (Jiang & Graham 1993).

To get an insight into the medium effect on the radiolysis mechanism, we would like to compare the yields of various species produced from the C_2H_2···CO complexes in different noble gas matrices. Roughly comparable conversion degrees of the parent complex were achieved (at the longest irradiation time) in all the matrices – ca. 40, 40, and 50 per cent in Ar, Kr, and Xe, respectively. As could be seen in Fig. 2, the amount of C_3O is comparable in Ar and Xe matrices while that of C_3O in a Kr matrix is noticeably higher. The amounts of HCCCHO and H_2CCCO decrease dramatically while coming from Ar to Kr and these products are absent in a Xe matrix. It may imply a high contribution of ionic channels to the production of HCCCHO and H_2CCCO since ionic channels are usually more efficient in an Ar matrix (Feldman 1999). The concentration of c-H_2C_3O has a non-monotonous dependence on matrix and increases in a row Kr < Xe < Ar. It was reported that c-H_2C_3O could be produced by the reaction of triplet excited acetylene with CO and vice versa (Zhou et al. 2008). Production of c-H_2C_3O through triplet states may account for higher efficiency of its formation in Xe as compared to Kr. Triplet states can be populated by electron–hole recombination or direct transition (due to spin–orbit interaction which is stronger in xenon due to the external heavy atom effect; Ryazantsev et al. 2018), which results in more efficient population of triplet states and, hence, more efficient formation of cyclopropenone. Very weak signals of HC_3O was observed in all the studied matrices (most intense – in Ar), so we cannot reliably investigate the matrix effect on its formation. Considering high intensity of the $CCCO_{asym\ str}$ absorption of HC_3O (1846 km mol^{-1} according to the CISD/6–311G* calculations; Cooksy et al. 1995), we conclude that this radical is a minor product of the radiation-induced transformations of the C_2H_2···CO complexes in noble gas matrices.

In order to understand the mechanisms of the radiation-induced transformations of the C_2H_2···CO complex, one should analyse the accumulation kinetics of radiolysis products. The corresponding build-up profiles for an Ar matrix are presented in Fig. 3 (curves for Kr and Xe matrices are provided on Fig. S3 and Fig. S4). For the comparative kinetic analysis, these build-up profiles for the various products of the C_2H_2···CO radiolysis are presented in invariant coordinates – relative intensity of product absorption (referred to as 'normalized concentration' below) versus reagent (i.e. the complex) conversion degree (Ryazantsev & Feldman 2015b). An intense $C{\equiv}O_{str}$ absorption band was used to trace the conversion degree of the complex.

The build-up profiles for the C_3O accumulation in Ar, Kr, and Xe matrix reveal an acceleration in the formation rate of this species with increasing absorbed dose. Similar effect is also observed for the HC_3O radical in an Ar matrix (build-up profiles for HC_3O in Kr and Xe matrices cannot be reliably obtained owing to the low intensity of its absorption in Kr and Xe) and for c-H_2C_3O in a Kr matrix and that implies the high contribution of a secondary reaction channels in the formation of these species. Accumulation of the H_2C_3O isomers in an Ar matrix flattens out (HCCCHO and c-H_2C_3O) or reach their maxima (H_2CCCO) at ca. 35 per cent of the parent complex conversion. In a Kr matrix, accumulation of HCCCHO and H_2CCCO tend to saturate even at lower conversion degree of the C_2H_2···CO complex (ca. 20 per cent). We can speculate

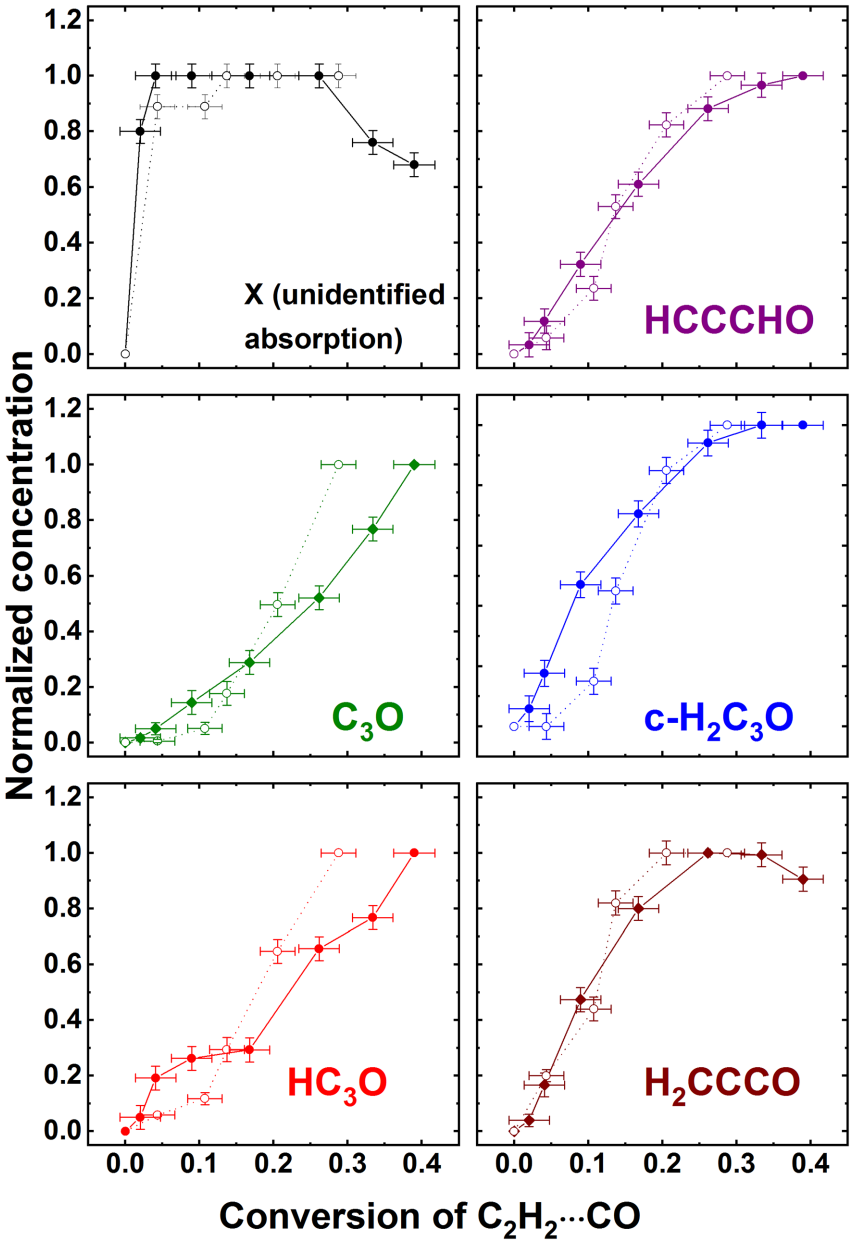

Figure 3. Accumulation profiles for radiolysis products of the C_2H_2···CO complex in an Ar matrix. Curves are provided for the $^{12}C_2H_2$/CO/Ar 1:3:1000 (solid lines, filled circles) and $^{13}C_2H_2$/CO/Ar 1:3:1000 (dotted lines, empty circles) samples. The C = O_{str} IR-absorption bands were integrated to determine the normalized concentrations of C_3O, HCCCHO, and H_2CCCO, while the bands corresponding to the $CCCO_{asym\ str}$ and $C–H_{wag\ in\text{-}plane}$ modes were used for HC_3O and c-H_2C_3O, respectively. **X** is unidentified carrier of the 2265.6 cm^{-1} ($^{12}C_2H_2$/CO/Ar) and 2263.7 cm^{-1} ($^{13}C_2H_2$/CO/Ar) absorptions.

that relatively high rate of decomposition of these H_2C_3O isomers in krypton may account for the observed higher yield of C_3O, as compared to other matrices. Accumulation of c-H_2C_3O in a Xe matrix saturates at a moderate conversion degree of the parent complex (ca. 50 per cent).

Linear accumulation for the H_2C_3O isomers in noble gas matrices at low irradiation doses presumably reveals that these species could be formed in one step. HCCCHO could be produced in one step from the excited stated of the C_2H_2···CO complex through dissociation of acetylene, intermediate formation of C_2H···HCO radical pair and its subsequent recombination (reaction 1). Another H_2C_3O isomer, c-H_2C_3O, as it was mentioned above, could be produced by the reaction of triplet excited acetylene with CO and vice versa (Zhou et al. 2008), which in our case would correspond to reaction 2. We assume that H_2CCCO could be generated in the same manner as propynal: through acetylene isomerization to H_2CC and subsequent recombination of the H_2CC···CO isolated pair (reaction 3). A formal scheme of these transformations can be represented as follows:

$$C_2H_2 \cdots CO \rightsquigarrow [C_2H \cdots HCO] \rightarrow HCCCHO \quad (1)$$

$$C_2H_2 \cdots CO \rightsquigarrow \text{c-}H_2C_3O \quad (2)$$

$$C_2H_2 \cdots CO \rightsquigarrow [H_2CC \cdots CO] \rightarrow H_2CCCO \quad (3)$$

The saturation of the H_2C_3O isomers accumulation kinetics at higher absorbed doses could be caused by their decomposition to the

parent complex or dehydrogenation to C_3O or/and HC_3O. It is worth noting that we did not observe the further degradation (decomposition of C_3O) under the conditions of our experiment as no traces of C_3 or C_2O (Jacox 2003) species were detected in the irradiated matrices.

The dose dependence for accumulation of C_3O and HC_3O in Ar, C_3O and c-H_2C_3O in Kr; and C_3O in Xe implies the existence of intermediate species on the reaction pathways of their formation. The formation of C_3O at low conversion degree of the parent complex C_2H_2···CO may be associated with involvement of 'direct' C_2H_2···CO → C_3O transformation, which probably occurs via a 'hot' intermediate, similar to the prompt CO formation in the case of methanol radiolysis in noble gas matrices (Saenko & Feldman 2016). In the case of Kr matrix, HCCCHO and H_2CCCO could probably be converted to C_3O by the radiation-induced dehydrogenation or into c-H_2C_3O by radiation-induced isomerization. It is worth noting that the efficiency of c-H_2C_3O formation in a Kr matrix is the lowest one, which may imply low efficiency of its direct formation. In other studied matrices, the efficiency of direct cyclopropenone production is probably higher due to its formation through ionic channel in Ar and triplet channel in Xe. Therefore, indirect cyclopropenone formation (e.g. via isomerization of other H_2C_3O isomers or via the transformation of an unidentified intermediate product) makes an important contribution to the total c-H_2C_3O production in the case of a Kr matrix (in contrast to Ar and Xe), which may account for a prominent acceleration of cyclopropenone formation in Kr and its absence in Ar and Xe matrices.

In a Xe matrix, the c-H_2C_3O molecules probably undergo transformation to C_3O at high absorbed doses as it could be concluded from the build-up profiles. In contrast, the build-up profiles for the H_2C_3O isomers in an Ar matrix exhibit a maximum (or flatten out) at rather high degrees of parent complex conversion, which makes questionable their role as intermediates in C_3O and HC_3O formation. However, in the case of X-irradiated $^{12}C_2H_2$/CO/Ar matrix, an absorption feature with maximum at 2265.6 cm^{-1} was found. It obviously belongs to an intermediate species (**X**) according to the kinetic behaviour of this band. The build-up profile for this species (see Fig. 3) demonstrates a maximum at ca. 5–25 per cent conversion degree of the parent complex. The FTIR spectra of an X-irradiated $^{12}C_2H_2$/CO/Ar matrix illustrating the dose-dependent accumulation of the radiolysis products are presented in Fig. S5. To note, the IR absorption feature with a maximum at 2263.7 cm^{-1} detected in the X-ray irradiated $^{13}C_2H_2$/CO/Ar matrices shows similar accumulation profile. We failed to detect any other absorption bands with the same kinetic behaviour in an Ar matrix or corresponding absorptions in Kr or Xe matrices. We may note that the unidentified absorption features at 2282.5 and 2265.4 cm^{-1} in Kr and 2269.2 cm^{-1} (with a shoulder at 2271.5 cm^{-1}) in Xe demonstrate prominent induction period (see Fig. S6), thus, from kinetic point of view, the carrier of these bands is not a primary intermediate produced directly from C_2H_2···CO (unlike the carrier of the bands attributed to species **X** in argon).

Based on the analysis of the accumulation profiles (Fig. 3) and available literature data (Brown et al. 1975; Brown et al. 1985; Chapman et al. 1987; Botschwina & Reisenauer 1991; Jiang & Graham 1993; Szczepanski et al. 1995; East 1998; Maier & Lautz 1998; O'Sullivan et al. 2007), we may conclude that the 2265.6 cm^{-1} feature does not belong to any of the considered C_3 products (C_3O, HC_3O, HCCCHO, H_2CCCO, and c-H_2C_3O). Moreover, an extensive theoretical study of the H_2C_3O potential energy surface (Ekern, Szczepanski & Vala 1996) does not reveal any H_2C_3O isomer, which could absorb in the marked IR region. However, we should also consider charged species because they are commonly formed under radiolysis. We are unaware of any reports on detection of the $H_2C_3O^-$ and HC_3O^- species. C_3O^- anion has no IR absorption in the considered spectral region according to the RCCSD(T) (FULL)/AVTZ calculations (Aoki 2011). We found that the yield of C_2H radical in the C_2H_2/CO/Ar matrices was noticeably lower than that in the C_2H_2/Ar matrices at similar conversion degrees of monomeric acetylene, while the yield of C_2H^- species was considerably higher. At the same time, the yield of Ar_2H^+ does not increase in the C_2H_2/CO/Ar matrices (as compared to C_2H_2/Ar). The increased yield of C_2H^- without increase of Ar_2H^+ amount implies that some cationic species is stabilized in the X-irradiated C_2H_2/CO/Ar matrices. Speculating of possible cationic intermediates, we may notice that the formation of the C_3O^+ cation as a primary intermediate would correspond to a single-step full dehydrogenation of the ionized acetylenic moiety of the complex, which looks unlikely due to its extremely high endothermicity (note that the radiation-induced formation of C_2 from acetylene in noble gas matrices is a two-step process demonstrating an induction period; Ryazantsev at al. 2018). Regarding the HC_3O^+ cation, it was detected by infrared predissociation action spectroscopy in combination with ion traps (Thorwirth et al. 2020) and its C = O_{str} frequency (2313 cm^{-1}) reasonably fits the absorption of **X** detected in our study in an Ar matrix (a matrix-induced shift of ca. 47 cm^{-1} seems plausible). On the other hand, the $H_2C_3O^+$ radical cation, which was reported to be a stable species (Bouchoux et al. 1986), could probably also absorb in the same IR spectral region. It is worth noting that the $H_2C_3O^+$ radical cation was considered earlier as an intermediate in the C_3O (one of the neutral radiolysis products detected in our experiments) formation pathway (Herbst et al. 1984), but no solid theoretical or experimental arguments were presented for this clue. Thus, we may assume that either HC_3O^+ or $H_2C_3O^+$ radical cations could be the species **X**. Detailed experimental and theoretical study of the $H_2C_3O^+$ radical cation deserves special attention, and it will be a subject of our further work. Here we confine ourselves to the assumption that this radical cation could probably be an important intermediate in the radiation-induced formation of various C_3 species in the C_2H_2–CO system.

The discussion given above provides a qualitative consideration focusing of possible genesis of different species appearing upon the X-radiolysis of matrix-isolated C_2H_2···CO complexes. We could mention that the formal procedure of global kinetic fitting based on the solution of coupled differential equations system was used previously for description of product kinetics in irradiated ultrathin films of neat and binary ices (see e.g. Zhou et al. 2008; Zhou et al. 2014). The application of such procedure to the decay of parent complex and kinetic evolution of key observed products in Kr and Xe matrices demonstrates qualitative validity of the proposed scheme (see Fig. S7 and Table S2). In the case of Ar matrix, the mechanistic scheme is probably more complicated because of significant role of an unidentified intermediate species **X** (presumably, cationic). We have to stress out that the global kinetic fitting approach should not be directly applied to the quantitative analysis of the systems studied in our work because of complexity of real processes and limited amount of available data. First, the radiation chemistry in matrices actually involves multichannel chemical reactions including both ionic and neutral excited states populated due to charge and/or excitation transfer from matrix to the studied complex (see Introduction and references cited therein). The presence of a number of unassigned bands may partially reflect this diversity. Furthermore, the efficiency of these processes in relatively thick matrix layers may change during the radiolysis due to modification of matrix/ice structure and morphology and production of new radiation-induced electron

traps (e.g. radicals). It is a typical complication for the so-called dispersive kinetics in solids manifested by significant deviation of the decay kinetics from simple exponential dependence, which is often treated in terms of the 'time-dependent rate constant' formalism yielding the stretched exponential kinetics: $n/n_0 = \exp(-kt^{\alpha})$, where $\alpha < 1$ (see Plonka 2001). The non-exponential decay of the parent complex in our experiments is illustrated by Fig. S8. Secondly, in any case, reliable fitting of the experimental data would require the knowledge of absolute or comparable relative concentrations of different products, which is unavailable because of lack of the corresponding absorption coefficients, and much larger number of experimental points because of large number of variable parameters.

4 ASTROCHEMICAL IMPLICATIONS AND COMPARISON WITH PREVIOUS EXPERIMENTS

In this work, we have demonstrated that both HCCCHO and c-C_3H_2O species can be formed in the cold radiation-induced transformations of the $C_2H_2\cdots CO$ complex. Formation of these compounds was observed previously in the electron-irradiated mixed C_2H_2–CO ices at 10 K (Zhou et al. 2008). Thus, one may expect that their synthesis could occur in the ice-coated interstellar grains processed with Galactic cosmic rays followed by their further release to the gas phase. Both propynal and cyclopropenone were found in the ISM: propynal was first observed in the cold cloud TMC-1 in 1988 (Irvine et al. 1988) and cyclopropenone was initially detected towards Sagittarius B2 (N) (Hollis et al. 2006).

In addition, the radiolysis of matrix-isolated 1:1 $C_2H_2\cdots CO$ complex also results in the formation of C_3O and HC_3O. The former molecule was found in the ISM (Irvine et al. 1984), but the latter one has not been detected so far. We have found that formation of HC_3O is a minor channel of the radiation-induced evolution in the binary $C_2H_2\cdots CO$ system (the yield of HC_3O in our experiments was, at least, an order of magnitude lower as compared to that of C_3O). Thus, non-efficient production and rather high reactivity of HC_3O (as compared to C_3O) may explain the non-detection of this radical in space. Returning to C_3O, this molecule seems to be the ultimate result of radiation-induced transformations of the matrix-isolated $C_2H_2\cdots CO$ complex (at least, at moderate absorbed doses). Regarding the most probable ways of its further transformations (to C_3O^+, C_3, C_3^+, HC_3O^+, and C_4^+; Urso et al. 2019), one may consider C_3O to be an exit point from the world of COM (potentially pre-biotic) to the flavourless world of non-organics. Meanwhile, it should be noted that the elongated carbon chain may be retained under prolonged radiolysis, so C_3O and species formed in its further transformations could be the next building block (considering the carbon skeleton as a basis) for the more complex interstellar species.

Considering propadienone, another product observed in our experiments, it is worth noting that H_2CCCO (being thermodynamically the most stable among the H_2C_3O isomers) has not been detected in the ISM so far. This fact represents a prominent example of the violation of the minimum energy principle (MEP) which states that the thermodynamically most stable species should be the most abundant (Lattelais et al. 2009). Generally speaking, the non-detection of H_2CCCO implies kinetic (rather than thermodynamic) control for production and destruction of the H_2C_3O isomers. In other words, there are some reactions that favour either production of cyclopropenone and propynal and/or the destruction of propadienone, but their identities remain mysterious (Shingledecker et al. 2019). Since H_2CCCO was detected in our experiments together with the other H_2C_3O isomers, the pathways of cold radiation-induced synthesis of H_2C_3O molecules from C_2H_2 and CO cannot explain the lack of interstellar cyclopropenone. Thus, reactions leading to the destruction of propadienone should be considered. Addition of atomic hydrogen to H_2CCCO resulting in destruction of propadienone in the gas-phase is expected to be barrierless and exothermic reaction and this may clarify the puzzle of the H_2CCCO non-detection (Shingledecker et al. 2019).

We also would like to compare the radiation chemistry of the matrix-isolated $C_2H_2\cdots CO$ complex with the radiation chemistry of mixed C_2H_2–CO ices (Zhou et al. 2008). Generally speaking, one may speculate that the CO-rich ices (CO matrices doped with acetylene) should bear some resemblance to the noble-gas media from the viewpoint of radiation chemistry. Indeed, the CO molecule is highly resistant to photon and electron radiation at the molecular level. On the other hand, the electronic properties of CO (such as ionization energy and polarizability influencing charge transfer and energy relaxation) are expected to be rather close to that of krypton. As it was mentioned in the Introduction, HCCCHO, c-H_2C_3O, HCO, and $HCCC_2H_3$ were observed in the irradiated mixed C_2H_2–CO ices at 10 K while H_2CCCO, C_3O, C_5O, and C_3O_2 were assigned only tentatively. Meanwhile, three last species were detected in irradiated low-temperature pure carbon monoxide ices (Jamieson, Mebel & Kaiser 2006), thus the role of acetylene in their formation is questionable. One can note that the most intense absorption of H_2CCCO is very close to absorption of CO (ca. 20 cm^{-1} difference), so we assume that overlapping of most intense H_2CCCO absorption with CO absorption in the irradiated C_2H_2–CO ices hindered the unambiguous H_2CCCO identification in the study of Zhou et al. (2008) and it is a plausible reason why the attributed H_2CCCO only tentatively (by a weak C–H_{str} absorption). This fact indicates an advantage of matrix isolation approach for the reliable detection of the radiolysis products using FTIR spectroscopy. Except $HCCC_2H_3$, C_5O and C_3O_2 (which cannot be formed from the 1:1 $C_2H_2\cdots CO$ complex owing to atomic balance conservation), all of the products detected in the irradiated C_2H_2–CO ices were observed in our matrix-isolation experiments. A rather high relative yield of H_2C_3O isomers in ices at the initial stages of radiolysis shows an important role of synthetic radiation chemistry of the C_2H_2–CO molecular pair in the evolution of ices containing both acetylene and carbon monoxide. It should be also noted that rather high irradiation doses are typically used in the experiments with mixed ices, so early radiolysis stages may be missed with consequent non-detection of important primary intermediates. In this work, in the C_2H_2/CO/Ar matrices we have directly detected the IR signatures of an intermediate species (most probably, $H_nC_3O^+$, $n = 1$ or 2, to be investigated in further studies) that is formed from $C_2H_2\cdots CO$ preceding the formation of the main radiation-induced products. No primary intermediates of that kind were detected in the electron-irradiated C_2H_2–CO ices (Zhou et al. 2008).

An interesting point is concerned with significant difference in the radiation-induced transformations of the $C_2H_2\cdots CO$ and $C_2H_2\cdots H_2O$ complexes. In fact, the matrix-isolated $C_2H_2\cdots H_2O$ complex (Zasimov et al. 2020a) demonstrates a water-mediated cleavage C≡C bond in acetylene. The bond cleavage occurs through the radiation-induced oxidation of acetylene by water yielding the H_2CCO–H_2 pair, which mainly transforms into CH_4 and CO (C_1 species) under further radiolysis. In contrast, the carbon skeleton of acetylene in the $C_2H_2\cdots CO$ complex is retained under irradiation and even growth with the addition of carbon monoxide: all of the observed radiolysis products are C_3 species. C_3O, the product of 'deep' radiolysis, was found to be quite radiation-resistant under conditions of our experiment, so one should expect this molecule to be the predominant

radiation-induced product in the C_2H_2–CO system at high absorbed doses. It implies the high stability of elongated carbon skeleton under the astrochemically relevant conditions. To sum up, the acetylene complexes demonstrate a remarkable diversity in the pathways of radiation-induced transformations.

5 SUMMARY AND CONCLUSIONS

In summary, we have demonstrated that the radiation-induced evolution of the 1:1 C_2H_2···CO intermolecular complex in a rigid inert environment at low temperatures results in the formation of COM such as the H_2C_3O isomers (propynal, cyclopropenone, and propadienone) as well as C_3O and HC_3O. The observed transformations provide a prominent direct proof of synthetic chemistry leading to elongation of a carbon chain within the isolated 'building block' of precursor under the conditions of completely frozen molecular mobility. This result appears to be crucially significant for elucidation of the mechanistic issues related to the processes in complex ices, particularly in the CO-based ices containing acetylene. Based on our results, we may suggest that the C_2H_2–CO mixed ices could be an important source both of interstellar cyclopropenone and propynal as well as interstellar C_3O. Propadienone can be also formed in the C_2H_2–CO ices under irradiation, so the non-detection of this molecule in the ISM remains puzzling.

Furthermore, the investigation of radiation chemistry of weak intermolecular complexes using a matrix isolation approach was demonstrated in this work to be a powerful tool for modelling the radiation-induced processes occurring in mixed interstellar ices and elucidation of their detailed mechanisms. We believe that this approach can be applied to unravel the mechanistic issues for other complex ices of astrochemical interest.

ACKNOWLEDGEMENTS

This work was supported by the Russian Foundation for Basic Research (project no. 19–03–00579-a). Experimental assistance from I.V. Tyulpina is gratefully acknowledged.

DATA AVAILABILITY

The data underlying this article are available in the article and in its online supplementary material.

REFERENCES

Abplanalp M. J., Kaiser R. I., 2019, Phys. Chem. Chem. Phys., 21, 16949
Abplanalp M. J., Kaiser R. I., 2020, ApJ, 889, 3
Adamowicz L., 1992, Chem. Phys. Lett., 192, 199
Allamandola L. J., 1987, J. Mol. Struct., 157, 255
Andrews L., Kushto G. P., Zhou M., Willson S. P., Souter P. F., 1999, J. Chem. Phys., 110, 4457
Aoki K., 2011, Adv. Space Res., 47, 2004
Arumainayagam C. R. et al., 2019, Chem. Soc. Rev., 48, 2293
Balucani N. et al., 2000, ApJ, 545, 892
Barclay A. J., Mohandesi A., Michaelian K. H., McKellar A. R. W., Moazzen-Ahmadi N., 2018, Mol. Phys., 116, 3468
Bennett C. J., Pirim C., Orlando T. M., 2013, Chem. Rev., 113, 9086
Botschwina P., Reisenauer H. P., 1991, Chem. Phys. Lett., 183, 217
Bouchoux G., Hoppilliard Y., Flament J. P., Terlouw J. K., Van der Valk F., 1986, J. Phys. Chem., 90, 1582
Brown F. R., Finseth D. H., Miller F. A., Rhee K. H., 1975, J. Am. Chem. Soc., 97, 1011
Brown R. D., Pullin D. E., Rice E. H. N., Rodler M., 1985, J. Am. Chem. Soc., 107, 7877
Carr J. S., Najita J. R., 2008, Science, 319, 5869,
Chapman O. L., Miller M. D., Pitzenberger S. M., 1987, J. Am. Chem. Soc., 109, 6867
Cherchneff I., Barker J. R., Tielens A. G. G. M., 1992, ApJ, 401, 269
Cooksy A. L., Tao F. M., Klemperer W., Thaddeus P., 1995, J. Phys. Chem., 99, 11095
Coustenis A. et al., 2007, Icarus, 1989
Contreras C. S., Salama F., 2013, ApJS, 208, 6
Cuylle S. H., Zhao D., Strazzulla G., Linnartz H., 2014, A&A, 570, A83
Dawes R., Wang X.-G., Carrington T., Jr, 2013, J. Phys. Chem. A, 117, 7612
Didriche K., Herman M., 2010, Chem. Phys. Lett., 496, 1
Dubost H., 1976, Chem. Phys., 12, 139
East A. L. L., 1998, J. Chem. Phys., 108, 3574
Ekern S., Szczepanski J., Vala M., 1996, J. Phys. Chem., 100, 16109
Feldman V. I., 2014, in Lund A., Shiotani M., eds., Application of EPR in Radiation Research. Springer, Cham, p. 151
Feldman V. I., Ryazantsev S. V., Saenko E. V., Kameneva S. V., Shiryaeva E. S., 2016, Radiat. Phys. Chem., 124, 7
Feldman V. I., 1999, Radiat. Phys. Chem., 55, 565
Forney D., Jacox M. E., Thompson W. E., 1992, J. Mol. Spectrosc., 153, 680
Germann T. C., Tschopp S. L., Gutowsky H. S., 1992, J. Chem. Phys., 97, 1619
Golovkin A. V., Davlyatshin D. I., Serebrennikova A. L., Serebrennikov L. V., 2013, J. Mol. Struct., 1049, 392
Herbst E., 2017, Int. Rev. Phys. Chem., 36, 287
Herbst E., Smith D., Adams N. G., 1984, A&A, 138, L13
Hollis J. M., Remijan A. J., Jewell P. R., Lovas F. J., 2006, ApJ, 642, 933
Hudson R. L., Moore M. H., 2003, ApJ, 586, L107
Hudson R. L., Loeffler M. J., 2013, ApJ, 773, 109
Hünig I., Oudejans L., Miller R. E., 2000, J. Mol. Spectrosc., 204, 148
Irvine W. M., Friberg P., Hjalmarson Å., Johansson L. E. B., Thaddeus P., Brown R. D., Godfrey P. D., 1984, Bull. Am. Astron. Soc., 16, 877
Irvine W. M. et al., 1988, ApJ, 335, L89
Jamieson C. S., Mebel A. M., Kaiser R. I., 2006, ApJS, 163, 184
Jacox M.E., 2003, J. Phys. Chem. Ref. Data, 32, 1
Jiang Q., Graham W. R. M., 1993, J. Chem. Phys., 98, 9251
Jovan Jose K. V., Gadre S. R., Sundararajan K., Viswanathan K. S., 2007, J. Chem. Phys., 127, 104501
Kaiser R. I., Roessler K., 1998, ApJ, 503, 959
Kameneva S. V., Tyurin D. A., Feldman V. I., 2016a, Radiat. Phys. Chem., 124, 30
Kameneva S. V., Tyurin D. A., Nuzhdin K. B., Feldman V. I., 2016b, J. Chem. Phys., 145, 214309
Kameneva S. V., Tyurin D. A., Feldman V. I., 2017a, Phys. Chem. Chem. Phys., 19, 24348
Kameneva S. V., Volosatova A. D., Feldman V. I., 2017b, Radiat. Phys. Chem., 141, 363
Kawashima Y., Nishizawa K., 1996, Chem. Phys. Lett., 253, 77
Khriachtchev L., 2015, J. Phys. Chem. A, 119, 2735
Kleimeier N. F., Abplanalp M. J., Johnson R. N., Gozem S., Wandishin J., Shingledecker C. N., Kaiser R. I., 2021, ApJ, 911, 24
Knez C. et al., 2008, in Kwok S., Sandford S., eds, Proc. IAU Symp. 251, Organic Matter in Space. Cambridge Univ. Press, Cambridge, p. 47
Knez C., Moore M. H., Ferrante R. F., Hudson R. L., 2012, ApJ, 748, 95
Ku H. H., 1966, J. Res. Natl. Bur. Stand., 70, 4
Kunttu H. M., Seetula J. A., 1994, Chem. Phys., 189, 273
Lahuis F., van Dishoeck E. F., 2000, A&A, 355, 699
Lacy J. H., Evans N. J., Achtermann J. M., Bruce D. E., Arens J. F., Carr J. S., 1989, ApJ, 342, L43
Lattelais M., Pauzat F., Ellinger Y., Ceccarelli C. 2009, ApJ, 696, L133
Lukianova M. A., Sanochkina E. V., Feldman V. I., 2019, J. Phys. Chem. A, 123, 5199
Lukianova M. A., Sosulin I. S., Tyurin D. A., Feldman V. I., 2020, Radiat. Phys. Chem., 176, 109022

Lukianova M. A., Volosatova A. D., Drabkin V. D., Sosulin I. S., Kameneva S. V., Feldman V. I., 2021, Radiat. Phys. Chem., 180, 109232
Marshall M. D., Prichard D. G., Muenter J. S., 1989, J. Chem. Phys., 90, 6049
Maier G., Lautz C., 1998, Eur. J. Org. Chem., 5, 769
Milligan D. E., Jacox M. E., 1969, J. Chem. Phys., 51, 277
Mumma M. J., Charnley S. B., 2011, ARA&A, 49, 471
Mumma M. J., DiSanti M. A., Russo N. D., Magee-Sauer K., Gibb E., Novak R., 2003, Adv. Space Res., 31, 2563
Öberg K. I., 2016, Chem. Rev., 116, 9631
O'Sullivan P. J., Livingstone R. J., Liu Z., Davies P. B., 2007, Mol. Phys., 105, 727
Pereira R. C., de Barros A. L. F., da Costa C. A. P., Oliveira P. R. B., Fulvio D., da Silveira E. F., 2020, MNRAS, 495, 40
Plonka A., 2001, Dispersive Kinetics, Springer Science & Business Media, Dordrecht, 234p
Rivera-Rivera L. A., McElmurry B. A., Wang Z., Leonov I. I., Lucchese R. R., Bevan J. W., 2012, Chem. Phys. Lett., 522, 17
Ryazantsev S. V., Feldman V. I., 2015a, J. Phys. Chem. A, 119, 2578
Ryazantsev S. V., Feldman V. I. 2015b, Phys. Chem. Chem. Phys., 17, 30648
Ryazantsev S. V., Tarroni R., Feldman V. I., Khriachtchev L., 2017, ChemPhysChem, 18, 949
Ryazantsev S. V., Zasimov P. V., Feldman V. I., 2018, Radiat. Phys. Chem., 151, 253
Ryazantsev S. V., Zasimov P. V., Feldman V. I., 2020, Chem. Phys. Lett., 753, 137540
Rutkowski K.S., Melikova S. M., Smirnov D. A., Rodziewicz P., Koll A., 2002, J. Mol. Struct., 614, 305
Saenko E. V., Feldman V. I., 2016, Phys. Chem. Chem. Phys.,18, 32503
Shingledecker C. N., Álvarez-Barcia S., Korn V. H., Kästner J., 2019, ApJ, 878, 80
Singh S. et al., 2016, ApJ, 828, 55
Sonnentrucker P., González-Alfonso E., Neufeld D. A., 2007, ApJ, 671, L37
Szczepanski J., Ektern S., Vala M., 1995, J. Phys. Chem., 99, 8002
Thorwirth S. et al., 2020, Mol. Phys., e1776409
Tielens A. G. G. M., Tokunaga A. T., Geballe T. R., Baas F., 1991, ApJ, 381, 181
Urso R. G. et al., 2019, A&A, 628, A72
Volosatova A. D., Kameneva S. V., Feldman V. I., 2019, Phys. Chem. Chem. Phys., 21, 13014
Whittet D. C. B., Bode M. F., Baines D. W. T., Longmore A. J., Evans A., 1983, Nature, 303, 218
Whittet D. C. B., Longmore A. J., McFadzean A. D., 1985, MNRAS, 216, 45P
Winnewisser G., Walmsley C. M., 1979, Ap&SS, 65, 83
Wu C. R., Judge D. L., Cheng B. M., Shih W. H., Yih T. S., Ip W. H., 2002, Icarus, 156, 456
Young N. A., 2013, Coord. Chem. Rev., 257, 956
Zack L. N., Maier J. P., 2014, Chem. Soc. Rev., 43 4602
Zasimov P. V., Ryazantsev S. V., Tyurin D. A., Feldman V. I., 2020a, MNRAS, 491, 5140
Zasimov P. V., Belousov A. V., Baranova I. A., Feldman V. I., 2020b, Radiat. Phys. Chem., 177, 109084
Zhou L., Kaiser R. I., Gao L. G., Chang A. H., Liang M. C., Yung Y. L., 2008, ApJ, 686, 1493
Zhou L., Maity S., Abplanalp L., Turner A., Kaiser R. I., 2014, ApJ, 790, 38

SUPPORTING INFORMATION

Supplementary data are available at *MNRAS* online.

Figure S1. Fragments of the FTIR spectra of the deposited C_2H_2/CO/Ng and C_2H_2/Ng matrices, Ng = Kr and Xe.
Figure S2. Fragments of the difference FTIR spectra of the X-irradiated C_2H_2/CO/Ng and C_2H_2/Ng matrices (Ng = Ar, Kr, and Xe) demonstrating vibronic bands of the C_2H radical.
Figure S3. Accumulation profiles for radiolysis products of the C_2H_2···CO complex in a Kr matrix.
Figure S4. Accumulation profiles for radiolysis products of the C_2H_2···CO complex in a Xe matrix.
Figure S5. Fragments of the difference FTIR spectra of a $^{12}C_2H_2$/CO/Ar (1:3:1000) matrix irradiated up to different doses.
Figure S6. Accumulation profiles for the absorptions observed in the 2260–2285 cm^{-1} region in different irradiated matrix samples.
Figure S7. Fitting of the kinetics of the C_2H_2···CO complex decomposition and build-up of the key radiolysis products in Kr and Xe matrices.
Figure S8. Kinetics of radiation-induced decomposition of the C_2H_2···CO complex in Ar, Kr, and Xe matrices.
Table S1. Summary of unassigned absorptions found in the FTIR spectra of the X-irradiated C_2H_2/CO/Ng matrices (Ng = Ar, Kr, and Xe).

Please note: Oxford University Press are not responsible for the content or functionality of any supporting materials supplied by the authors. Any queries (other than missing material) should be directed to the corresponding author for the article.

This paper has been typeset from a Microsoft Word file prepared by the author.